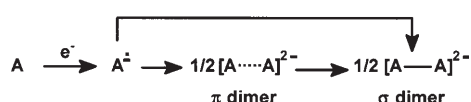


# Evidence for a $\pi$ Dimer in the Electrochemical Reduction of 1,3,5-Trinitrobenzene: A Reversible $N_2$ -Fixation System\*\*

Iluminada Gallardo,\* Gonzalo Guirado, Jordi Marquet, and Neus Vilà

Couplings between two radical anions<sup>[1]</sup> or two radical cations<sup>[2]</sup> are common outcomes in electrochemical reactions and give rise to a doubly charged  $\sigma$ -bonded dimeric species. In the case of delocalized  $\pi$  systems such as 9-cyanoanthracene, formation of a  $\pi$ -dimer intermediate before collapse of the two radical anions into a  $\sigma$ -bonded species has been proposed,<sup>[2a-b]</sup> although the same event has been explained by one-step radical-anion dimerization<sup>[2c-d]</sup> (Scheme 1).



Scheme 1. Dimerization of the radical anion of 9-cyanoanthracene (A).

Moreover, the formation of radical-anion dimers in the solid state, such as that of 7,7,8,8-tetracyanoquinodimethane (TCNQ), is well established.<sup>[3]</sup> Furthermore, it is known that the nucleophilic aromatic substitution ( $S_NAr$ ) mechanism involves addition compounds ( $\sigma$  complexes) as intermediates.<sup>[4]</sup> For this reaction, UV and NMR spectroscopic experiments suggested the existence of a  $\pi$ -complex intermediate prior to  $\sigma$ -complex formation.<sup>[5]</sup> Definitive evidence was provided by the isolation of the  $\pi$ -complex intermediate in the  $S_NAr$  reaction of indole-3-carboxylate with 1,3,5-trinitrobenzene.<sup>[6]</sup> Thus, the formation of  $\pi$ -dimer intermediates in the  $\sigma$  dimerization of radical anions remains controversial.

In the reduction of 1,3,5-trinitrobenzene (**1**), Bock and Lechner-Knoblauch observed an irreversible wave, which was explained by formation of 1,3-dinitrobenzene and nitrite anion.<sup>[7]</sup> However, by bulk electrochemical reduction of **1** in acetone, Sosokin et al. isolated the  $\sigma$ -bonded dimer 1,1'-

dihydrobis(2,4,6-trinitrocyclohexadienyl) (**3**, Scheme 2) as its tetraethylammonium salt.<sup>[8]</sup> We report herein on a complete electrochemical (cyclic voltammetry and bulk electrolysis), spectroscopic, and synthetic investigation of the reduction of **1**, providing conclusive evidence for the formation of a  $\pi$ -dimer intermediate prior to formation of the  $\sigma$  dimer and the reaction of this  $\pi$  dimer with  $N_2$  to give an organic  $N_2$ -fixation system.

The electrochemical behavior of **1** is definitely different from those of nitrobenzene or dinitrobenzenes (see the Supporting Information).<sup>[9]</sup> Figure 1a shows that, at low scan rates, **1** has one chemically irreversible reduction wave at  $-0.56$  V versus SCE in acetonitrile ( $CH_3CN$ ,  $0.1M$   $nBu_4NBF_4$ , Ar atmosphere,  $10^\circ C$ ). The resulting follow-up product is oxidized at  $+0.23$  V. This oxidation wave only appears after a first reduction scan. The reduction wave becomes reversible at scan rates higher than  $1800$   $Vs^{-1}$  ( $E^\circ = -0.57$  V,  $k_s = 0.01$   $cm s^{-1}$ ). Peak-potential analysis of the reduction wave at low and high scan rates indicates a one-electron process. The shape of the voltammograms (peak width) suggests fast electron transfer with kinetic control by chemical reaction.<sup>[10]</sup> The peak potential is concentration-dependent ( $22$  mV per unit  $\log c$ ) and scan rate-dependent ( $23$  mV per unit  $\log v$ ) in the concentration range  $2$ – $10$  mM. These cyclic voltammetric data indicate dimerization of the radical anion of **1** through a second-order reaction pathway ( $[E + C2(Arr)]$  mechanism) to form **2**, which is responsible for the oxidation wave at  $+0.23$  V (Scheme 2).<sup>[11]</sup> A dimerization rate constant of  $k_2 = (1.80 \pm 0.05) \times 10^5$   $L mol^{-1} s^{-1}$  was determined by simulation of the experimental curves with the DigiSim software.<sup>[12]</sup>

Dianion **2** was synthesized as its tetraethylammonium salt ( $Et_4N$ )<sub>2</sub>-**2** by bulk electrolysis of **1**. A fresh solution of this salt in  $CH_3CN$  ( $0.1M$   $nBu_4NBF_4$ , Ar,  $10^\circ C$ ) shows, at low scan rates, a two-electron process for the characteristic oxidation peak at  $+0.23$  V. The characteristic reduction peak of **1** at  $-0.56$  V is observed only after the potential is set above  $+0.23$  V (Figure 1b), which means that the oxidation product of **2** is **1**. Furthermore, **1** is recovered in 100% yield after exhaustive electrolysis of **2** at  $+0.40$  V. If the cyclic voltammogram is recorded 5 min after preparing the solution, a new oxidation peak rises at  $+0.56$  V, while the height of the peak at  $+0.23$  V decreases in comparison with the initial value. In less than one hour, only the peak at  $+0.56$  V remains in the cyclic voltammogram, and the peak at  $+0.23$  V is no longer visible. This new peak at  $+0.56$  V is assigned to **3** (Scheme 2).

The tetraethylammonium salt of dianion **3** was isolated and characterized by aging a solution of **2** in  $CH_3CN$ .<sup>[13]</sup> A freshly prepared solution of the salt of **3** in  $CH_3CN$  ( $0.1M$   $nBu_4NBF_4$ , Ar atmosphere,  $10^\circ C$ ) shows, at low scan rates, a

[\*] Dr. I. Gallardo, Dr. G. Guirado, Prof. J. Marquet, Dr. N. Vilà  
Departament de Química  
Universitat Autònoma de Barcelona  
08193 Bellaterra, Barcelona (Spain)  
Fax: (+34) 93-581-2920  
E-mail: iluminada.gallardo@uab.es

[\*\*] We gratefully acknowledge the financial support of the Ministerio de Tecnología y Ciencia of Spain through projects BQU 2003-05457 and CTQ2006-01040. We also thank Dr. C. P. Andrieux and Prof. J. Pinson for the availability of spectroelectrochemical facilities, Prof. C. Sieiro and Prof. P. J. Alonso for EPR experiments, Prof. J. P. Dinnocenzo, Dr. C. Flaschenriem, Dr. T. Roisnel, and Dr. Á. Álvarez for X-ray diffraction data/structure determination, and all of them for helpful discussions.

Supporting information for this article is available on the WWW under <http://www.angewandte.org> or from the author.

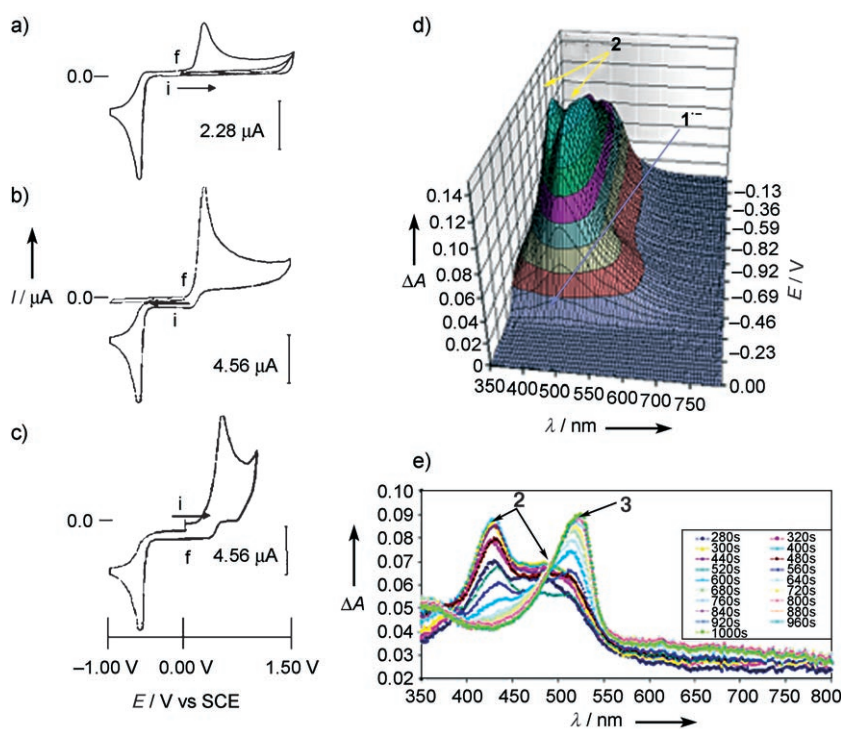
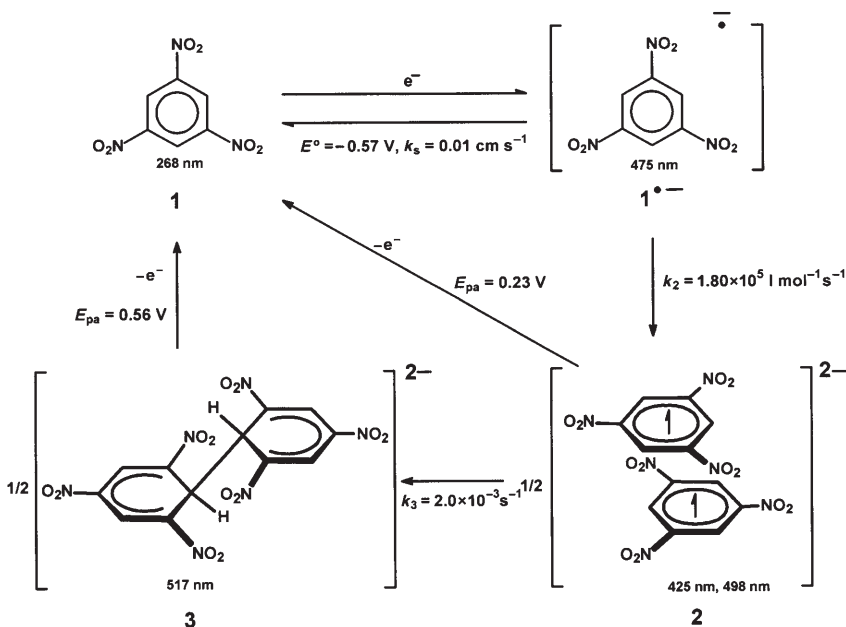


**Figure 1.** Cyclic voltammety (CV) at 4.0 mm in  $\text{CH}_3\text{CN}$  with 0.1 M  $n\text{Bu}_4\text{NBF}_4$  at  $10^\circ\text{C}$ . Scan rate  $1.0\text{ V s}^{-1}$ , glassy carbon disk electrode (0.05 mm diameter). a) **1** in the potential range 0.00/1.50/−1.00/0.00 V (two cycles). b) **2** in the potential range 0.00/−1.00/1.50/0.00 V (two cycles). c) **3** in the potential range 0.00/1.00/−1.00/0.00 V. d) Spectroelectrochemical plot of **1** (0.5 mM) with scan rate  $0.1\text{ V s}^{-1}$  in the potential range 0.00/−1.00/0.00 V; 60 spectra were recorded during the scan.<sup>[15]</sup> e) In situ UV/Vis spectra during electrolysis of **1** (0.5 mM) at −1.00 V vs.  $\text{Ag}/\text{AgCl}$  in a spectroelectrochemical cell with Pt minigrad as working electrode.<sup>[15]</sup>



**Scheme 2.** Detailed mechanism for reduction of **1** under an Ar atmosphere.

two-electron oxidation process for the peak at +0.56 V (Figure 1c). Again, the characteristic reduction peak of **1** at −0.56 V only arises after the oxidation of **3**, which indicates

that **1** is the oxidation product of **3**. This is corroborated by exhaustive electrolysis (+1.30 V) of **3**, which gives **1** in 100% yield. The oxidation peak of **3** (+0.56 V) is in the range of oxidation potentials found for the  $\sigma$  complexes formed in  $\text{S}_{\text{N}}\text{Ar}$  reactions (0.60–1.00 V),<sup>[14]</sup> whereas **2** is oxidized at a lower potential (+0.23 V), which is consistent with a  $\pi$  dimer.

A potential-step experiment in a UV/Vis–electrochemical cell<sup>[15]</sup> facilitates measuring the disappearance of **2** by monitoring the absorption band at 425 nm and the appearance of a new band at 517 nm (Figure 1e; for technical details, see the Supporting Information).<sup>[16]</sup> From these data, it is possible to deduce that the absorption of **2** (425 and 498 nm) grows rapidly in the beginning, while **1** is totally consumed (about 400 s). Later, the absorption bands of **2** decrease, with concomitant development of the new absorption of **3** (517 nm). Highly accurate kinetic data, gathered by monitoring the appearance of the new absorption band at 517 nm over time, led to  $k_3 = 2 \times 10^{-3}\text{ s}^{-1}$  for the isomerization process **2**→**3** (see the Supporting Information).

The tetraethylammonium salt of dianion **2** was synthesized as a paramagnetic crystalline solid by electrolyzing a solution of **1** in  $\text{CH}_3\text{CN}$  under argon with  $\text{Et}_4\text{NBF}_4$  as supporting electrolyte.<sup>[17]</sup> The needle-shaped, conducting crystals grew on a graphite cathode (Figure 2).

X-ray analysis of **2** shows a  $\pi$ -stacked structure in the solid state (Figure 3).<sup>[18]</sup> The radical-anion units are not parallel to each other; instead, the stack shows a smooth zigzag motif through a short contact (2.48(3) Å) between C2 of one unit and C4<sup>i</sup> ( $i: -x, y + 1/2, -z + 1/2$ ) of the next. The dihedral angle between the mean planes of two neighboring units is  $34.5(8)^\circ$  and the ring slippage is 1.85(3) Å. This tilted structure could be preserved in solution until the shortest C–C distance collapses to give a  $\sigma$  bond when  $\pi$  dimer **2** evolves into **3**.

Furthermore, **2** is a biradical in solution, as shown by the EPR spectrum of frozen DMF solutions (77 K) of **2** (see the Supporting Information). The spectrum is the result of an  $S = 1$  entity having axial symmetry with an isotropic  $g$  factor ( $g = 2.0075 \pm 0.0005$ ) and a zero-field splitting parameter of  $D = 323.1 \pm 0.5\text{ MHz}$ .<sup>[19]</sup> The central signal corresponds to a two-photon  $\Delta M_s = \pm 2$  transition.<sup>[20]</sup> Moreover, solutions of the paramagnetic species **2** in  $\text{CH}_3\text{CN}$  show fluorescence ( $\lambda_{\text{emission}} = 608\text{ nm}$ ,  $\Phi = 0.25$ , irradiation at 428 nm; see the Supporting Information).<sup>[21]</sup> Neither fluorescence nor an EPR signal was observed for  $\sigma$  complex **3**.

When the electrochemical reduction of **1** is performed in  $\text{N}_2$  atmosphere instead of Ar, neither the oxidation waves of **2** (+0.23 V vs. SCE) nor those of **3** (+0.56 V vs. SCE) are observed in the cyclic voltammogram.

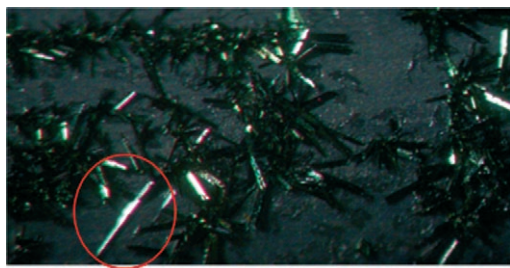


**Figure 2.** Crystal growing on the graphite electrode surface when electrolysis of **1** is performed at  $-0.60$  V.

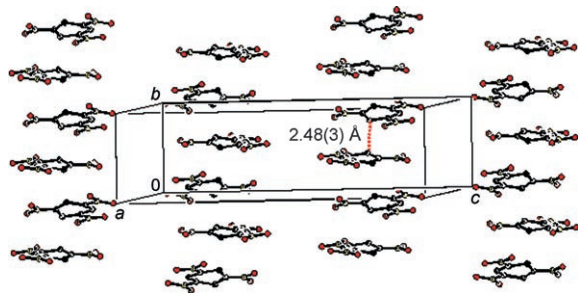


**Figure 3.** Crystal structure of  $(\text{Et}_4\text{N})_2 \cdot 2$ . The dashed line shows the shortest distance between two aromatic rings  $\text{C}2 \cdots \text{C}4^i$  ( $i: -x, y + 1/2, -z + 1/2$ ). Tetraethylammonium counterions are omitted for clarity.

However, a new oxidation wave occurs at  $+1.09$  V versus SCE and corresponds to a two-electron transfer process (Figure 4). By analogy with the electrochemical behavior of **1** under Ar, the oxidation wave at  $+1.09$  V can be assigned to dimer **4**. This species was quantitatively formed in solution by electrolysis of **1** at  $-0.60$  V versus SCE (20 mM,  $\text{CH}_3\text{CN}$ ,  $0.1$  M  $n\text{Bu}_4\text{NBF}_4$ ,  $\text{N}_2$ ) after passing 1 F. The electrogenerated species again shows an oxidation wave at  $1.09$  V versus SCE. The characteristic reduction peak of **1** at  $-0.56$  V is observed only after the potential is set above  $+1.09$  V (Figure 1a), that is, the oxidation product of **4** is **1**. Furthermore, **1** is recovered in a 100% yield after exhaustive electrolysis of **4** at  $+1.20$  V (Scheme 3, path B).

To establish whether the new species **4** arises from the reaction of **2** or **3** with  $\text{N}_2$ , the tetraethylammonium salt of **2** was dissolved in  $\text{CH}_3\text{CN}$  and a flow of nitrogen was

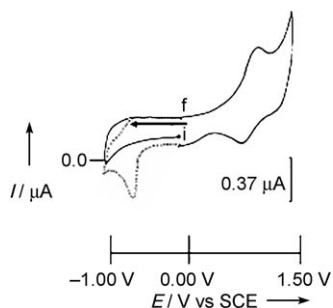
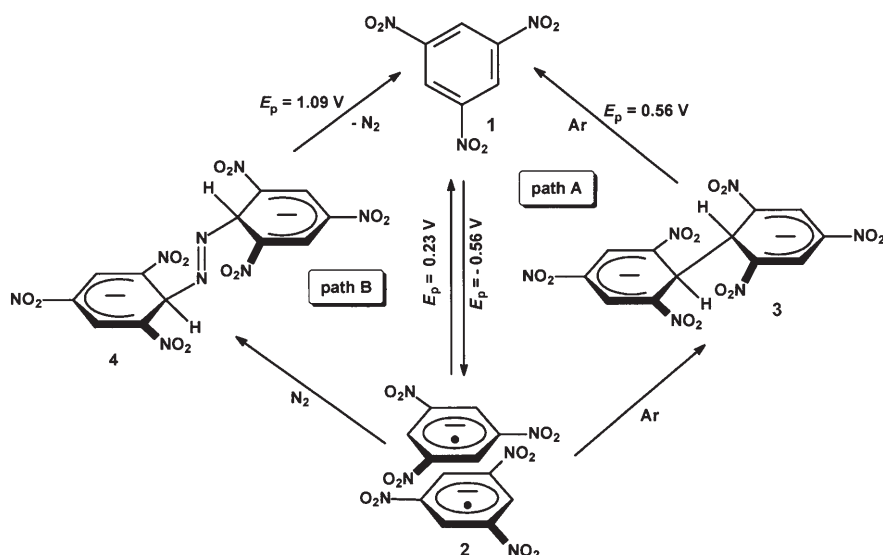


**Figure 4.** CV of  $(\text{Et}_4\text{N})_2 \cdot 4$  (0.5 mM) in  $\text{CH}_3\text{CN}$  with  $0.1$  M  $n\text{Bu}_4\text{NBF}_4$  at  $10^\circ\text{C}$ . Scan rate  $1.0$   $\text{Vs}^{-1}$ , glassy carbon disk electrode ( $\varnothing$  0.5 mm). The potential ranges were  $0.00/-1.00/1.50/0.00$  V (first scan, solid line) and  $0.00/-1.00/0.00$  V (second scan, dotted line).

immediately passed through the solution and maintained for 10 min. Electrochemical analysis of the resulting solution showed an identical  $I-E$  curve to that of electrogenerated **4**, that is, a two-electron oxidation wave at  $+1.09$  V. The fact that no difference was observed when  $\text{N}_2$  was bubbled through a solution of **3** unequivocally showed that the new product **4** arises from the reaction of biradical **2** with one molecule of  $\text{N}_2$  (Scheme 3, path B). Further evidence for this composition was provided by electrospray-ionization mass spectrometry (ESI<sup>+</sup>) analysis of an electrogenerated solution of the tetraethylammonium salt of **4**; the peaks at  $713.4$   $[\text{M}-\text{H}]^-$ ,  $357.2$   $[\text{M}]^{2-}$ , and  $213.0$   $[\text{M}-28]^{2-}$  show appropriate isotopic distribution.

All attempts to isolate a salt of **4** by direct electrochemical reduction of **1** under  $\text{N}_2$  failed. However, we were able to isolate single crystals of the tetraethylammonium salt of **4** by exposing the green crystals of the tetraethylammonium salt of **2** to an  $\text{N}_2$  flow for one week. This unusual solid-gas reaction at room temperature affords the tetraethylammonium salt of **4** as a red-orange crystalline material. A fresh solution of these crystals in  $\text{CH}_3\text{CN}$  under Ar shows an identical CV to electrogenerated solutions of **4**. The  $^1\text{H}$  NMR spectrum of **4** shows two singlets at  $\delta = 8.40$  and  $6.41$  ppm (2:1), which are significantly shifted with respect to those of the  $\sigma$  complex **3** at  $\delta = 8.15$  and  $5.53$  ppm.

The molecular structure of dianion **4** is shown in Figure 5.<sup>[22]</sup> It consists of two trinitrobenzene units linked by an azo group through two  $\text{sp}^3$  carbon atoms (C6 and C12). Thus, the C6–C1, C6–C5, C12–C7, and C12–C11 bonds (av  $1.484(3)$  Å) are longer than the remaining C–C distances in the rings. Furthermore, distances between the  $\text{sp}^2$  carbon atoms are consistent with a quinonic structure for the rings, since C1–C2, C4–C5, C7–C8, and C10–C11 are significantly shorter (av  $1.358(5)$  Å) than C2–C3, C3–C4, C8–C9, and C9–C10 (av  $1.402(3)$  Å). The C–N distances are within the normal range, but the N=N distance ( $1.481(5)$  Å) is longer than those reported for other azo compounds. Moreover, the angles around the azo fragment are severely distorted: the C6–N14–N13 and C12–N13–N14 angles are only  $107.5(3)^\circ$  and  $107.3(3)^\circ$ , respectively, and the dihedral angle around the N=N bond (C6–N14–N13–C12) is  $131.5(4)^\circ$ . All these structural data indicate significant single-bond character for this azo bond. Interestingly, each of the nitrogen atoms lies within a short, nonbonding distance of two oxygen atoms of two *ortho*-nitro groups (N13 $\cdots$ O62  $3.046(7)$ , N14 $\cdots$ O11  $3.028(5)$  Å). Since the oxygen atoms carry a significant fraction of the negative charge of the dianion, donation from these atoms into the  $\pi^*$  bond of the N=N fragment cannot be ruled out. This could be the reason for the observed N=N bond lengthening, as well as the pyramidalization around the N atoms. The close resemblance between the packings of the structures of **2** and **4** suggests that dinitrogen molecules diffuse into solid **2** and bind two neighboring trinitrobenzene radicals without making major changes in the crystal structure or changing the space group. However, the two trinitrobenzene fragments in **4** are no longer related by crystallographic symmetry. Therefore, the volume of the unit cell of **4** ( $3434(2)$  Å<sup>3</sup>) is about twice that of **2** ( $1646.4(5)$  Å<sup>3</sup>). Furthermore, the symmetry elements in the crystal are



**Scheme 3.** Mechanism for the reversible dimerization of **1** under Ar (path A) or N<sub>2</sub> (path B).

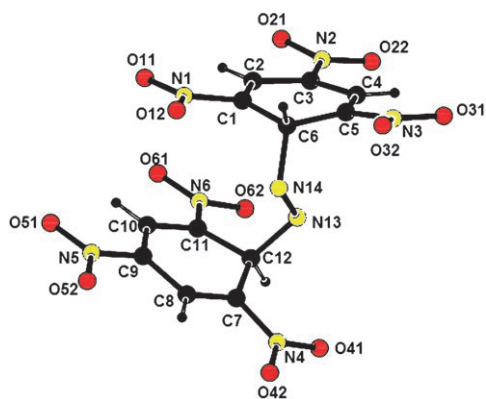


**Figure 5.** Molecular structure of dianion **4**.<sup>[22]</sup>

rearranged between **2** and **4**. While in **2** the  $\pi$  stack of trinitrobenzene molecules runs along a  $2_1$  axis, parallel to the crystallographic  $b$  axis, the column of azo dimers in **4** is generated by a  $c$ -glide plane parallel to the  $c$  axis (Figure 6).

In summary, the radical anion of **1** dimerizes to form biradical  $\pi$  dimer **2**, which forms a  $\pi$ -stacked structure in the solid state. The reversible conversion between the monomeric and dimeric species (**2** and **3**) provides a new example of a molecular switch (Scheme 3, path A) under Ar atmos-

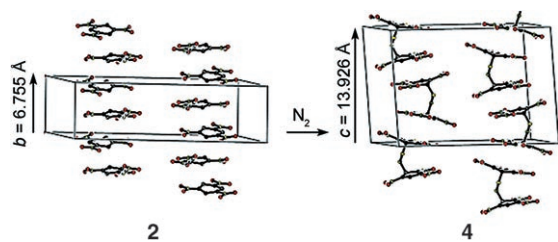


**Figure 6.** Comparison of the unit cells of the tetraethylammonium salts of **2** and **4**. Cations are omitted for clarity.

phere.<sup>[23]</sup> Whereas there are numerous examples of dinitrogen coordinating to transition metal systems,<sup>[24]</sup> we have shown for the first time that an organic molecule, namely, **2**, can reversibly bind N<sub>2</sub> at room temperature in an electrochemically controlled process under N<sub>2</sub> atmosphere (Scheme 3, path B). The different behaviors of the reduction product of 1,3,5-trinitrobenzene (**1**) under N<sub>2</sub> or an inert gas such as Ar provides the basis for building sensor devices for dinitrogen.

Received: July 6, 2006

Revised: October 25, 2006

Published online: December 29, 2006

**Keywords:** azo compounds · electrochemistry · nitrogen fixation · radicals · stacking interactions

- [1] a) M. M. Baizer, H. Lund, *Organic Electrochemistry*, Dekker, New York, **1983**; b) L. Nadjó, J. M. Savéant, D. Tessier, *J. Electroanal. Chem.* **1975**, *64*, 143; c) L. A. Avaca, J. H. P. Utley, *J. Chem. Soc. Perkin Trans. 1* **1975**, 971; d) M. Sertel, A. Y. Rolf-Gambert, H. Baumgärtel, *Electrochim. Acta* **1986**, *31*, 1287; e) C. P. Andrieux, A. Battle, M. Espin, I. Gallardo, Z. Jiang, J. Marquet, *Tetrahedron* **1994**, *50*, 6913; f) I. Gallardo, G. Guirado, J. Marquet, *J. Electroanal. Chem.* **2000**, *488*, 64; g) R. E. Del Sesto, A. M. Arif, J. S. Miller, *Chem. Commun.* **2001**, 2730; h) R. E. Del Sesto, A. M. Arif, J. J. Novoa, I. Anusiewicz, P. Skurski, J. Simons, B. C. Dunn, E. M. Eyring, J. S. Miller, *J. Org. Chem.* **2003**, *68*, 3367.
- [2] a) O. Hammerich, V. D. Parker, *Acta Chem. Scand. Ser. B* **1983**, *37*, 379; O. Hammerich, V. D. Parker, *Acta Chem. Scand. Ser. B* **1983**, *37*, 851; b) O. Hammerich, V. D. Parker, *Acta Chem. Scand. Ser. B* **1981**, *35*, 341; c) C. Amatore, J. Pinson, J. M. Saveant, *J. Electroanal. Chem.* **1982**, *137*, 143; d) J. M. Saveant, *Acta Chem. Scand. Ser. B* **1983**, *37*, 365; e) A. Smie, J. Heinze, *Angew. Chem.* **1997**, *109*, 375; *Angew. Chem. Int. Ed. Engl.* **1997**, *36*, 363; f) H. Yang, A. J. Bard, *J. Electrochem. Soc.* **1991**, *87*, 306; g) C. P. Andrieux, I. Gallardo, M. Junca, *J. Electroanal. Chem.* **1993**, *354*, 231; h) P. Bäuerle, U. Segelbacher, K. U. Gauld, D. Huttenlocher, M. Mehring, *Angew. Chem.* **1993**, *105*, 125; *Angew. Chem. Int. Ed. Engl.* **1993**, *32*, 76; i) J. Heinze, C. Willmann, P. Bäuerle, *Angew. Chem.* **2001**, *113*, 2936; *Angew. Chem. Int. Ed.* **2001**, *40*, 2861; j) V. Mazine, J. Heinze, *J. Phys. Chem. A* **2004**, *108*, 230.
- [3] a) M. C. Grossel, S. C. Weston, *Chem. Mater.* **1996**, *8*, 977; b) Similar types of  $\sigma$  dimers, and occasionally  $\pi$  dimers, have been reported for related compounds, such as tetracyanoethylene (TCNE) derivatives: J. S. Miller, *Angew. Chem.* **2006**, *118*, 2570; *Angew. Chem. Int. Ed.* **2006**, *45*, 2508.
- [4] a) F. Terrier, *Nucleophilic Aromatic Displacement; The Influence of the Nitro Group*, *Organic Nitro Chem. Ser.* (Ed.: H. Feuer), VCH, New York, **1991**; b) E. Buncl, M. R. Crampton, M. J. Strauss, F. Terrier, *Electron Deficient Aromatic- and Heteroaromatic-Base Interactions*, Elsevier, Amsterdam, **1984**; c) G. A. Artamkina, M. P. Egorov, I. P. Beletskaya, *Chem. Rev.* **1982**, *82*, 427; d) F. Terrier, *Chem. Rev.* **1982**, *82*, 77; e) E. Buncl, *The Chemistry of Functional Groups. Supplement F. The Chemistry of Amino, Nitro and Nitroso Compounds* (Ed.: S. Patai), Wiley, London, **1982**.
- [5] a) R. Bacaloglu, C. A. Bunton, G. Cerichelli, *J. Am. Chem. Soc.* **1987**, *109*, 621; b) R. Bacaloglu, A. Blasko, C. A. Bunton, E. Dorwin, F. Ortega, C. Zucco, *J. Am. Chem. Soc.* **1991**, *113*, 238;

- c) R. Bacaloglu, A. Blasko, C. A. Bunton, F. Ortega, C. Zucco, *J. Am. Chem. Soc.* **1992**, *114*, 7708; d) R. Bacaloglu, C. A. Bunton, F. Ortega, *Int. J. Chem. Kinet.* **1988**, *20*, 195; e) R. Bacaloglu, C. A. Bunton, G. Cerichelli, F. Ortega, *J. Am. Chem. Soc.* **1988**, *110*, 3495.
- [6] P. Sepulcri, R. Goumont, J. C. Hallé, R. Buncel, F. Terrier, *Chem. Commun.* **1997**, 789.
- [7] H. Bock, U. Lechner-Knoblauch, *Z. Naturforsch.* **1985**, *40b*, 1463.
- [8] I. M. Sosonkin, A. Ya. Kaminskii, S. S. Gitis, V. A. Subbotin, Yu. D. Grudtsyn, *Zh. Obshch. Khim.* **1971**, *41*, 2579.
- [9] In all scans, nitrobenzene shows a one-electron reversible reduction wave, and dinitrobenzene two successive one-electron reversible reduction waves.
- [10] "Electrochemical Reactions in Investigation of Rates and Mechanism of Reactions": C. P. Andrieux, J.-M. Savéant in *Techniques of Chemistry, Vol. 6* (Ed.: C. F. Bernasconi), Wiley, New York, **1986**, chap. 2.1.
- [11] C. P. Andrieux, *Pure Appl. Chem.* **1994**, *66*, 2445.
- [12] Simulations were performed by using DIGISIM software, which is commercially available from BAS Corp.
- [13] a) The tetraethylammonium salt of 1,1'-dihydro-bis(2,4,6-trinitrocyclohexadienyl) dianion (**3**) was isolated and characterized as the same compound previously described by Sosokin et al.<sup>[8]</sup> Elemental analysis, UV/Vis spectroscopy (517 nm), <sup>1</sup>H NMR (the spectrum shows two singlets at  $\delta = 8.15$  and 5.53 ppm (2:1), corresponding to the two different kinds of protons). Importantly, no signals were observed by EPR or fluorescence techniques;<sup>[13b]</sup> b) Investigations by Taylor and Farnham under different environmental conditions showed that the fluorescence quantum yields of  $\sigma$  complexes are about 0.09 (S. Farnham, R. Taylor, *J. Org. Chem.* **1974**, *39*, 2446).
- [14] Recent results have shown that the oxidation potential of  $\sigma$  complexes are in the range of 0.60–1.00 V: a) I. Gallardo, G. Guirado, J. Marquet, *Chem. Eur. J.* **2001**, *7*, 1759; b) I. Gallardo, G. Guirado, J. Marquet, *ES2179727*, **2003**; c) I. Gallardo, G. Guirado, J. Marquet, *Eur. J. Org. Chem.* **2002**, 251; d) I. Gallardo, G. Guirado, J. Marquet, *Eur. J. Org. Chem.* **2002**, 261; e) I. Gallardo, G. Guirado, J. Marquet, *J. Org. Chem.* **2002**, *67*, 2548.
- [15] a) A. Neudeck, L. Dunsch, *J. Electroanal. Chem.* **1995**, *386*, 135; b) A. Neudeck, L. Kress, *J. Electroanal. Chem.* **1997**, *437*, 141.
- [16] a) The spectra of **1** and **3** show maximum absorption at 268 and 517 nm, respectively, in accordance with the literature;<sup>[4a,8]</sup> b) The maximum absorption of **2** was determined in our laboratory.
- [17] The tetraethylammonium salt of biradical bis(1,3,5-trinitrobenzene) dianion **2** was obtained by cathodic electrolysis of **1**. Potential-controlled electrolysis at  $-0.60$  V vs. SCE of **1** (20 mM, CH<sub>3</sub>CN, 0.1 M Et<sub>4</sub>NBF<sub>4</sub>, Ar, 10 °C) quantitatively produces **2** on a graphite working electrode after passage of 1 F. This dark green solid was isolated as a tetraethylammonium salt. Elemental analysis (%) of **2**, calculated for a dimeric structure (C<sub>28</sub>H<sub>46</sub>N<sub>8</sub>O<sub>12</sub>): N 16.37, C 48.98, H 6.71; found: N 15.94, C 48.60, H 6.72.
- [18] a) Crystal structure analysis of (Et<sub>4</sub>N)<sub>2</sub>-**2** (C<sub>14</sub>H<sub>23</sub>N<sub>4</sub>O<sub>6</sub>,  $M_r = 343.36$  g mol<sup>-1</sup>): A green needle was rapidly mounted under Paratone-8277 on a glass fiber and immediately placed in a cold nitrogen stream at  $-80$  °C on a Bruker diffractometer with SMART CCD area detector. Crystal size 0.28 × 0.05 × 0.03 mm; monoclinic, space group  $P2_1/c$ ;  $a = 11.657(2)$ ,  $b = 6.7546(14)$ ,  $c = 23.262(4)$  Å,  $\beta = 115.988(7)^\circ$ ,  $V = 1646.4(5)$  Å<sup>3</sup>,  $Z = 4$ ;  $\rho_{\text{calcd}} = 1.671$  g cm<sup>-3</sup>;  $\mu = 0.109$  mm<sup>-1</sup>;  $2\theta_{\text{max}} = 56.6^\circ$ ,  $\lambda(\text{MoK}\alpha) = 0.71073$  Å. 9295 reflections collected (1535 unique reflections,  $R_{\text{int}} = 0.1131$ ). Data were corrected for absorption with the SADABS<sup>[18b]</sup> program. The structure was solved by direct methods and refined (218 parameters) by full-matrix least-squares techniques on  $F^2$  (Bruker-AXS, SHELXTL-NT<sup>[18c]</sup> version 5.10). All non-hydrogen atoms were refined with anisotropic displacement parameters. Hydrogen atoms were included in idealized positions. The structure was refined to goodness-of-fit and final agreement factors of  $\text{GoF} = 1.211$ ,  $R1(I > 2\sigma(I)) = 0.1086$ ,  $wR2(\text{all data}) = 0.2376$ , residual electron density  $\pm 0.39$  e<sup>-</sup> Å<sup>-3</sup>. CCDC-616742 contains the supplementary crystallographic data for this paper. These data can be obtained free of charge from The Cambridge Crystallographic Data Centre via [www.ccdc.cam.ac.uk/data\\_request/cif](http://www.ccdc.cam.ac.uk/data_request/cif); b) The SADABS program is based on the Blessing method: R. H. Blessing, *Acta Crystallogr. Sect. A* **1995**, *51*, 33; c) SHELXTL NT: Structure Analysis Program, version 5.10, Bruker-AXS, Madison, WI, **1995**.
- [19] a) J. A. Weil, J. R. Bolton, J. E. Wertz, *Electron Paramagnetic Resonance: Elementary Theory and Practical Applications*, Wiley, New York, **1994**; b) to our knowledge, only one solid biradical has been obtained by photolysis: c) K. Mukai, T. Tamaki, *J. Chem. Phys.* **1978**, *68*, 2006.
- [20] a) J. W. Orton, P. Auzins, J. E. Wertz, *Phys. Rev. Lett.* **1960**, *4*, 128; b) J. W. Orton, P. Auzins, J. H. E. Griffiths, J. E. Wertz, *Proc. Phys. Soc. London Sect. A* **1961**, *78*, 554; c) M. S. de Groot, J. H. van der Waals, *Physica* **1963**, *29*, 1128; d) G. A. Ward, B. K. Coger, M. Findlay, J. C. W. Chien, *Inorg. Chem.* **1974**, *13*, 614; e) G. J. Zinder, D. A. Dougherty, *J. Am. Chem. Soc.* **1985**, *107*, 1774; f) D. Collison, M. Helliwell, V. M. Jones, F. E. Mabbs, E. J. L. Mc Innes, P. C. Riedi, G. M. Smith, R. G. Pritchard, W. I. Cross, *J. Chem. Soc. Faraday Trans.* **1998**, *94*, 3019; g) P. J. van Dam, A. A. K. Klaassen, E. J. Reijerse, W. R. Hagen, *J. Magn. Reson.* **1998**, *130*, 140.
- [21] a) M. A. Muñoz, O. Sama, M. Galán, P. Guardado, C. Carmona, M. Balón, *Spectrochim. Acta Part A* **2001**, *57*, 1049; b) the fluorescence quantum yield of **2** in CH<sub>3</sub>CN was determined in relation to the fluorescence quantum yield of *N',N'',N'''*-triisopropyl-4-oxo-6-isopropyliminio-2*s*-(2*H*)-triazinespiro-1',2',4',6'-trinitrocyclohexadienylide (0.5); c) in CH<sub>3</sub>CN, a compound with similar features: R. O. Al-Kaysi, G. Guirado, E. J. Valente, *Eur. J. Org. Chem.* **2004**, 3408.
- [22] Crystal structure analysis for (Et<sub>4</sub>N)<sub>2</sub>-**4** (C<sub>28</sub>H<sub>46</sub>N<sub>10</sub>O<sub>12</sub>,  $M_r = 714.75$  g mol<sup>-1</sup>) was performed on a Nonius Kappa CCD diffractometer. Crystal size 0.16 × 0.07 × 0.05 mm; monoclinic, space group  $P2_1/c$ ;  $a = 13.131(5)$ ,  $b = 19.359(5)$ ,  $c = 13.926(5)$  Å,  $\beta = 104.043(5)^\circ$ ,  $V = 3434(2)$  Å<sup>3</sup>,  $Z = 4$ ;  $\rho_{\text{calcd}} = 1.382$  g cm<sup>-3</sup>;  $\mu = 0.109$  mm<sup>-1</sup>;  $2\theta = 54.7^\circ$ ;  $\lambda(\text{MoK}\alpha) = 0.71073$  Å,  $T = 293(2)$  K. 42967 reflections collected (7606 unique reflections,  $R_{\text{int}} = 0.1286$ ). The structure was solved by direct methods and refined (452 parameters) by full-matrix least-squares methods on  $F^2$  with the SHELXTL package.<sup>[18c]</sup> Hydrogen atoms were calculated and placed in idealized positions. The structure was refined to goodness-of-fit and final agreement factors of  $\text{GoF} = 1.023$ ,  $R1(I > 2\sigma(I)) = 0.1058$ ,  $wR2(\text{all data}) = 0.3592$ , residual electron density  $+0.86$  and  $-0.32$  e<sup>-</sup> Å<sup>-3</sup>. CCDC-195183 contains the supplementary crystallographic data for this paper. These data can be obtained free of charge from the Cambridge Crystallographic Data Centre via [www.ccdc.cam.ac.uk/data\\_request/cif](http://www.ccdc.cam.ac.uk/data_request/cif).
- [23] a) Switching can be repeated more than 250 times.<sup>[2i,23b]</sup> Since **2** evolves spontaneously into **3**, the system can be considered a dynamic switch combining chromic and magnetic outputs; b) R. Rathore, P. Le Magueres, S. V. Lindeman, J. K. Kochi, *Angew. Chem.* **2000**, *112*, 818; *Angew. Chem. Int. Ed.* **2000**, *39*, 809.
- [24] M. Hidai, Y. Mizobe, *Chem. Rev.* **1995**, *95*, 1115.